Multistability and phase-space structure of dissipative nonlinear parametric four-wave interactions

J. C. P. Coninck, S. R. Lopes, and R. L. Viana
Departamento de Física, Universidade Federal do Paraná, 81531-990, Curitiba, Paraná, Brazil
(Received 29 April 2004; published 10 November 2004)

We investigate the phase-space structure displayed by a system of four waves interacting by means of nonlinear coupling between two wave triplets, which results in a dissipative high-dimensional vector field presenting an invariant manifold, wherein the dynamics is essentially conservative. The focus is on the coexistence of a large number of periodic attractors in the phase space, with an interwoven structure of the basins of attraction, where low-period attractors have predominance. The time behavior of nearly conserved quantities and the properties of the Lyapunov spectra are used to imply the existence of a lower-dimensional invariant manifold where the dynamics is nearly conservative. A three-dimensional map is used to illustrate these findings.

DOI: 10.1103/PhysRevE.70.056403 PACS number(s): 52.35.Mw, 05.45.−a

I. INTRODUCTION

A rather common feature of many physical systems is the saturation of linear instabilities by nonlinear saturation [1–4]. The understanding of such saturation mechanisms represents a fundamental physical problem. These kinds of analyses are, in general, difficult tasks. However, the analysis can be simplified in cases when linearly unstable systems consist of just few modes as, for example, nonlinear three and four wave interactions [5]. For problems of wave coupling displaying quadratic nonlinearity, interactions involving three or four modes may describe key features of turbulence in systems close to equilibrium [6]. Nonlinear wave-wave interactions occur in many physical examples in plasma physics and nonlinear optics. Some of the applications of nonlinear parametric wave interactions are anomalous laser absorption and laser beam filamentation in laboratory plasmas [7], auroral radio emissions [8], and solar wind modulation in space plasmas [9], second-harmonic production, amplification, frequency up-conversion, and phase-conjugation of optical signals [10], wave mixing in chiral liquids [11], generation of soft x rays by conversion of visible laser [12] and production of Raman waves (lasers) using dielectric microcavity [13]. Coherent four wave interactions appears also in nonlinear atom optics (interacting Bose-Einstein condensates) [14]. Parametric wave interaction plays an important role in conversion of incoherent light into coherent light as well [15,16].

Parametric wave-wave interactions of three and four wave is among the most widely studied wave-mixing or wave interaction configurations. It can be understood as a parametric amplification process where energy is transferred from a pump wave into two or three other waves [16]. Mathematically, such interaction processes can be described by a system of coupled-mode nonlinear differential equations which exhibit a wide variety of dynamical phenomena, from periodic to chaotic behavior, being also one of the oldest physical applications of nonlinear dynamics and chaos [3,4,16].

The case of dissipative three-wave coupling was shown to present transition to chaotic behavior through well-known routes, as a cascade of period-doubling bifurcations of cycles [17], and intermittency, where stable periodic orbits abruptly take over chaotic attractors [18]. These analyses can be further extended for certain classes of four-wave parametric interactions, in which two waves participate simultaneously in two resonant triplets [19,20]. The conservative case of this problem was found to be exactly integrable, since it presents the same number of integrals of motion as the degrees of freedom, when the wave frequencies match exactly [21]. When there is some frequency mismatch, however, the conservative four-wave interaction is no longer integrable. In this case, there has been found another scenario for transition to chaotic motion via separatrix chaos [22,23] : a solitonlike solution (separatrix) has been obtained for the integrable case, i.e., with perfect frequency matching. This solitonic solution becomes irregular with small frequency mismatch and, as the latter is increased the separatrix chaotic layer spreads along the phase space, eventually engrossing most of it [23].

Most analytical and numerical results on four-wave parametric interactions have focused on the conservative case. The dissipative case, however, when there is a frequency mismatch, still presents many hitherto unexplored features. For example, what is the fate of the periodic (Poincaré-Birkhoff) islands, and which represent resonances of the conservative system [24], when a small dissipation is introduced? Can those solitonlike solutions, found the integrable case, survive to dissipation, i.e., are they robust features of the theoretical model? Do chaotic orbits persist in presence of dissipation, and in what measure? Another important topic to mention is the fact that how a linearly unstable system can be stabilized (presenting saturated states) by nonlinear coupling [6]. In plasma physics, for example, many works have been done on wave interactions handling just linear growth rates. In spite of those works being useful, many of such results can be explained in more detail when the nonlinear case is studied. In fact many new results on nonlinear dynamics have brought better explanations about some physical systems (see [16] and references therein). These are some of the questions we address in this paper, which presents the

dissipative version of the four-wave parametric interaction model, with an invariant manifold, where the dynamics is conservative.

The results we show in this paper are consistent with general features expected for damped near-integrable Hamiltonian systems, for which the absence of an energy surface foliated in invariant tori leads to qualitatively different dynamics. In particular, those linear centers related to Poincaré-Birkhoff islands become multiple coexisting attractors with an involved basin structure due to the fractal nature of the basin boundaries [25]. The latter, on their hand, are responsible for the appearance of transient chaos, which represents most of the irregular dynamics, since the presence of chaotic attractors (and the corresponding basins of attraction) is rare in comparison with periodic attractors [26].

A key result of our analysis is the existence of an invariant manifold, embedded in the phase space of the system, to which the phase trajectories are attracted for large times. The dynamics on this manifold is conservative, since it preserves an energylike constant as time evolves; and the dissipative effects are found in the directions transversal to this invariant manifold. Since the full phase space of the wave-wave interaction problem is high-dimensional, these features can be better observed in a lower-dimensional mapping which possesses such an invariant manifold, and which retains many of the dynamical features of the physical system we are investigating.

The rest of the paper is organized as follows: in Sec. II we present the basic equations of the four-wave interaction model, together with a discussion of the phase space structure. Section III presents numerical evidences of the existence of an invariant manifold, as a subset of the phase space to which trajectories asymptote, and on which the dynamics is nearly conservative. Section IV treats the observed multistability, or the coexistence of a large number of periodic attractors, with an involved basin structure. These facts are best illustrated in Sec. V with the help of a low-dimensional mapping, which preserves some of the essential dynamical features found in the four-wave interaction problem. Our conclusions are left to the final section.

II. PHASE SPACE STRUCTURE

The resonant four-wave parametric interaction is comprised by the coupling of two three-wave sets, with the following phase-matching conditions (a schematic representation of this coupling being depicted in Fig. 1):

$$\omega_3 = \omega_1 - \omega_2 - \delta_3', \tag{1}$$

$$\omega_4 = \omega_1 + \omega_2 - \delta_4', \tag{2}$$

$$\mathbf{k}_3 = \mathbf{k}_1 - \mathbf{k}_2, \tag{3}$$

$$\mathbf{k}_4 = \mathbf{k}_1 + \mathbf{k}_2, \tag{4}$$

where $\delta_{3,4}'$ are the frequency mismatches for each of the wave triplets. We use the modulational notation for the wave fields

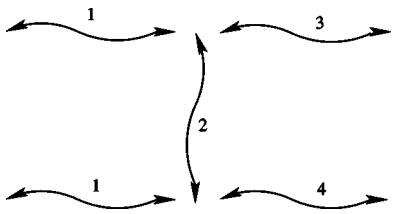

FIG. 1. Scheme of the four-wave interaction.

$$\mathbf{E}_\alpha(\mathbf{x},t) = \frac{1}{2}\mathcal{E}_\alpha(t)e^{i(\mathbf{k}_\alpha\cdot\mathbf{x}-\omega_\alpha t)} + \text{c.c.} \quad (\alpha = 1,2,3,4), \tag{5}$$

where $\mathcal{E}_\alpha(t)$ is a slowly varying complex envelope.

Not far from the threshold of the linear instability, or in other words, when the energy level of saturated states is sufficiently low [27] dynamical behavior of the four wave coupling in a quadratic nonlinear dissipative system can be described combining Maxwell's equations with the fluid equations and the linear dispersion relation $\omega_\alpha(\mathbf{k}_\alpha)$ of each interacting wave. Doing that we are able to derive normalized complex amplitudes for the envelopes:

$$A_\alpha(t) = f_\alpha\mathcal{E}_\alpha(t) = \text{Re}(A_\alpha) + i\ \text{Im}(A_\alpha) = |A_\alpha|e^{i\phi_\alpha} \quad (\alpha = 1,2,3,4), \tag{6}$$

where f_α are functions of the frequencies and dispersion operators (see [23] for explicit expressions for a particular case). In terms of these normalized complex amplitudes, the equations of the resonant parametric four-wave coupling are

$$\frac{dA_1}{dt} = A_2A_3 - rA_2^*A_4 + \nu_1A_1, \tag{7}$$

$$\frac{dA_2}{dt} = -A_1A_3^* - rA_1^*A_4 + \nu_2A_2, \tag{8}$$

$$\frac{dA_3}{dt} = -A_1A_2^* + i\delta_3A_3 + \nu_3A_3, \tag{9}$$

$$\frac{dA_4}{dt} = rA_1A_2 - i\delta_4A_4 + \nu_4A_4, \tag{10}$$

where $\delta_3 > 0$ and $\delta_4 > 0$ are the normalized linear frequency mismatches, $r > 0$ is the coupling parameter between triplets, $\nu_1 > 0$ is the linear energy injection coefficient, and $\nu_2 < 0$, $\nu_3 < 0$, and $\nu_4 < 0$ are dissipation parameters. Here we are assuming nonlinear coefficients equal to the unity since we have also normalized the wave amplitudes. In fact in many physically interesting cases, such coefficients will be complex, but the use of renormalized variables can make these coefficients real and limited [6] such that without loss of generality we are assuming them equal to the unity.

Since each wave field is characterized by two real parameters (amplitude $|A_i|$ and phase ϕ_i), they are out of eight variables in this system, such that its phase space is 8-dimensional. Let us first consider the conservative case ($\nu_1 = \nu_2 = \nu_3 = \nu_4 = 0$). In this case, the phase-space dimension can be substantially reduced thanks to conserved quantities

of the physical system which lead to integrals of motion, from the dynamical point of view. The first of these is the Hamiltonian, or energy function

$$H(A_i) = A_1A_2^*A_3^* - A_2A_3A_1^* + r(A_1^*A_2^*A_4 - A_1A_2A_4^*) + i(\delta_4|A_4|^2 - \delta_3|A_3|^2), \tag{11}$$

from which there results the following canonical equations for the wave amplitudes and their conjugate variables:

$$\frac{dA_i}{dt} = -\frac{\partial H}{\partial A_i^*}, \tag{12}$$

$$\frac{dA_i^*}{dt} = \frac{\partial H}{\partial A_i}. \tag{13}$$

Other conserved quantities, called c_1 and c_2, are given by the so-called Manley-Rowe relations:

$$c_1(A_i) = |A_1|^2 + |A_3|^2 + |A_4|^2, \tag{14}$$

$$c_2(A_i) = |A_1|^2 - |A_3|^2 + |A_4|^2. \tag{15}$$

These three integrals of motion reduce the phase space dimension from eight to five. This number can be further decreased, by two units, by using the phase conjugacies given by the Stokes and anti-Stokes modes

$$\phi_+ = \phi_1 + \phi_2 - \phi_4, \tag{16}$$

$$\phi_- = \phi_1 - \phi_2 - \phi_3 \tag{17}$$

and we have just three phase space dimensions, which can be readily studied by using a 2-dimensional Poincaré surface of section map. The structure of the phase space, in this case, has been investigated already [23].

Now if we let the dissipation coefficients ν_i have nonzero values, the former integrals of motion will be, in general, no longer conserved with time. The time rate of change of the phase space volume, which is the divergence of the vector field (7)–(10), which is given by

$$\mathcal{J} = \sum_{i=1}^{4} \frac{\partial \dot{A}_i}{\partial A_i} = 2\sum_{i=1}^{4} \nu_i, \tag{18}$$

is a constant value, indicating that the system is globally dissipative (antidissipative), i.e., the volumes shrink (expand) with time at the same rate everywhere in the available regions of the phase space. Since there are no longer conserved quantities, the only dimensional reduction we can make, in the dissipative case, is to use the phase conjugacies (16) and (17), which reduce the phase space dimension from eight to six. In the following, we will set $\nu_1 = 1.0$, $\nu_2 = \nu_3 = \nu_4 = -0.8$, and $r = 1.0$; such that $\mathcal{J} < 0$. We also define a symmetry-breaking parameter

$$\Delta = \delta_3 - \delta_4, \tag{19}$$

which measures the total mismatch between triplets. In other words, the value taken on by Δ gives us a measure of how efficient is the energy transport from one wave to another, interacting in each wave triplet.

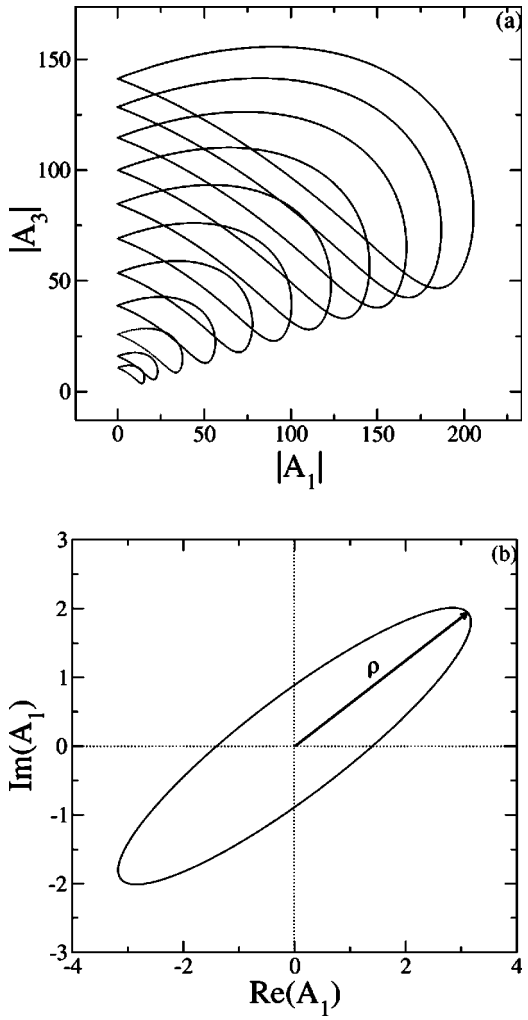

FIG. 2. (a) Multiple coexisting period-1 attractors in the $|A_3|$ versus $|A_1|$ projection of the phase space; (b) definition of a mean radius for a limit-cycle attractor.

As we shall see, when $\Delta = 0$ (symmetric case), the dynamics is strongly dissipative along four out of the six phase-space dimensions, which directs trajectories asymptotically to a two-dimensional manifold $\mathcal{M}$. The dynamics in this manifold can be parametrized by any set of suitable coordinates. We choose to work with the field amplitudes $|A_i|$ and $\mathrm{Re}(A_i)$. Figure 2(a) shows a projection of the phase space trajectories on the $|A_1|$-$|A_3|$ plane, in which a variety of different attracting closed orbits are shown (the apparent crossing of the trajectories is due to the projection we made), corresponding to different initial conditions.

The perspective view shown in Fig. 2(a) suggests a "funnel" with its vertex at the origin $|A_1| = |A_3| = 0$ and projecting out along the remaining phase space dimensions (mainly two of them, due to the existence of the manifold $\mathcal{M}$), the closed orbits being cross sections of it. Moreover, the fact that the system dynamics is effectively two-dimensional rules out the possibility of chaotic motion. These closed orbits have a complicated structure for their basins of attraction. In order to label the different attractors we can define a "mean radius" of such curves, $\rho(A_1)$, as illustrated by Fig. 2(b). If $\Delta = 0$, it is possible to find cycles with any value of the mean radius.

These limit cycles are thought to belong to a dense set of closed orbits.

III. CONSERVATIVE INVARIANT MANIFOLD

The large phase space dimension (six, effectively out of eight) of our four-wave system seems to hamper a more profound dynamical analysis. High-dimensional conservative dynamics in the energy surface can be extremely complicated due to factors as Arnold diffusion and stochastic pumping [28]. Nevertheless, the dissipative case can be simpler in the sense that the number of possible stationary states will decrease, as the dissipation builds up. Moreover, chaotic dynamics is mainly of a transient nature, since chaotic attractors would have attraction basins comparatively smaller than periodic attractors, and the latter dominate the dynamics [25].

The shrinking of phase space volume caused by dissipation helps us to simplify the system dynamics in another perspective. Globally dissipative systems have the property that a sphere of finite volume located in any point of the phase space will shrink into a zero-volume region. In the four-wave case, global dissipation leads phase-space volumes to a low-dimensional manifold on which the dynamics is almost conservative for the symmetric case ($\Delta=0$).

A numerical evidence for this assertion is depicted in Fig. 3(a), where we plot the time variation of the numerical value of the quantity H given by Eq. (11) for the dissipative case. We remark that H is no longer the Hamiltonian but, as soon as we reach the conservative manifold, H becomes constant (for $\Delta=0$). Such a fact enables us to define H for the dissipative case as an energy function which is conserved as the dynamics is restricted to the conservative manifold. In the conservative case ($\nu_i=0$) the energy function is rigorously conserved. On the other hand, in the dissipative case, and when the mismatch Δ is different from zero, the temporal evolution of H displays, after a transient time, small oscillations which indicate that the energy function is not conserved. In other words, the conservative invariant manifold ceases to exist in the latter situation.

Further evidence is given by Figs. 3(b) and 3(c), where we plot the time variation of the quantities c_1 and c_2 which, in the conservative case, are strictly constant, thanks to the Manley-Rowe relations (14) and (15). Note that, while H and c_2 are constant for $\Delta=0$, the quantity c_1 presents a bounded and regular oscillation about a fixed value. Such results show us that the dynamics in the invariant manifold preserved just the quantities H and c_2. In particular the former is conserved outside the manifold $\mathcal{M}$.

The dynamics in this manifold $\mathcal{M}$ is conservative thanks to the asymptotic convergence of the former integral of motion H into a constant value. Since these quantities (H and c_2) do not alter their value as time increases, we can imagine that this is an invariant manifold, since a trajectory that once reaches $\mathcal{M}$ will remain there for all time. The two-dimensional character of $\mathcal{M}$ is inferred from the Lyapunov spectrum of this model, shown in Fig. 4, where all the six Lyapunov exponents are depicted as a function of time. They are all strictly nonpositive, indicating absence of chaotic behavior. While four exponents are negative, we have two exponents equal to zero (in the symmetric case $\Delta=0$), indicating that the trajectories are pushed to this manifold along the remaining four directions in phase space (due to the correspondingly negative exponents).

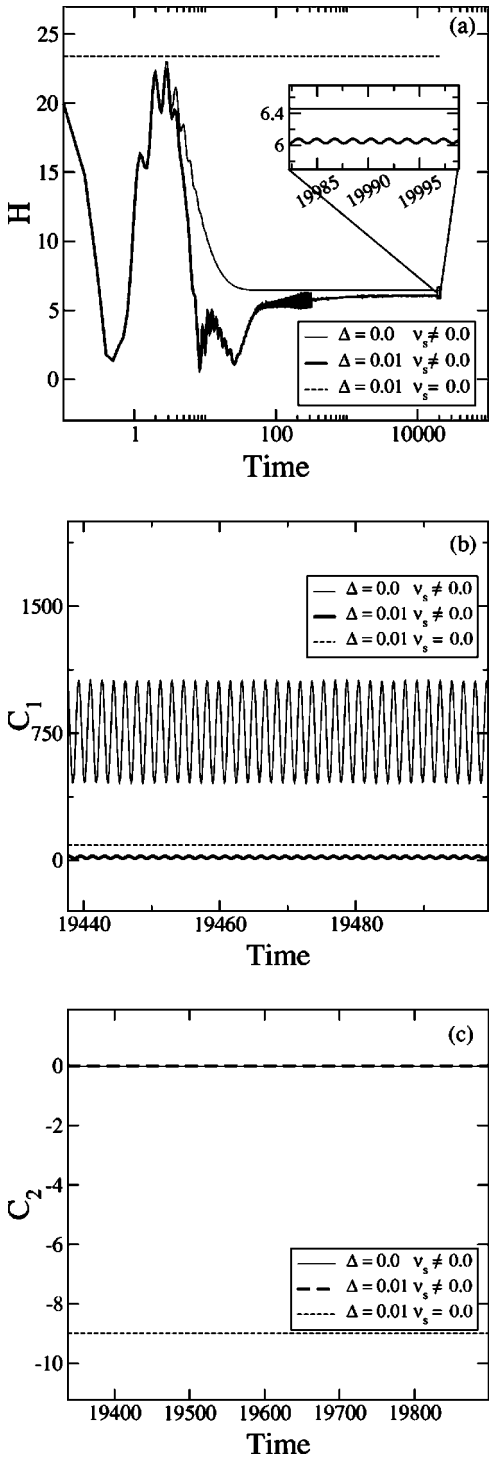

FIG. 3. Time evolution of the (a) energy function H; and the Manley-Rowe functions: (b) c_1 and (c) c_2, for $\Delta=0$ and $\Delta=0.01$.

For the $\Delta\neq 0$ case, such conservative invariant manifold does not exist at all, as we can see from the variation of the energy function $H(t)$ [Fig. 3(a)] and the Lyapunov spectrum

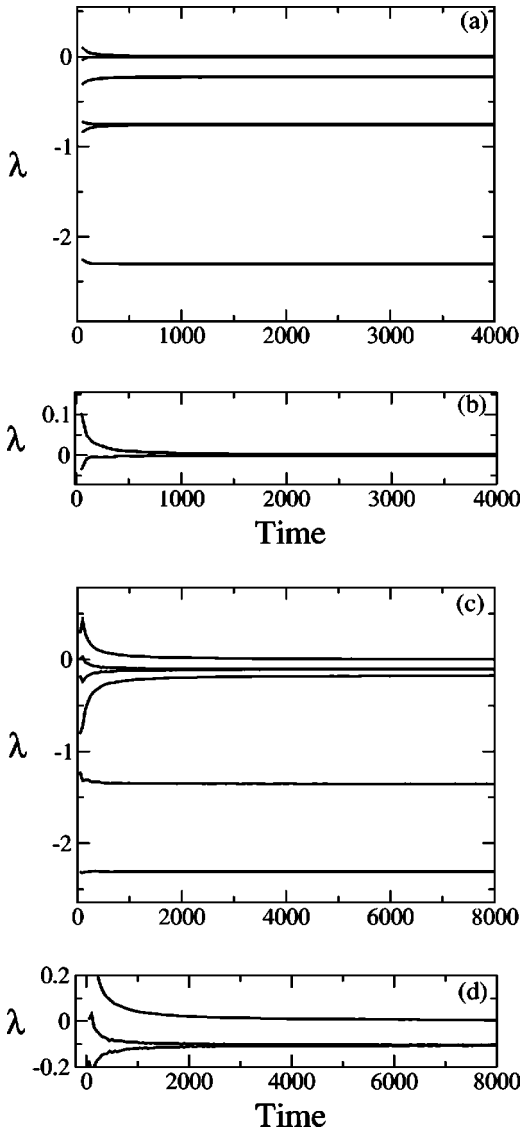

FIG. 4. Time evolution of the Lyapunov exponents for the resonant four-wave parametric interaction for (a) $\Delta=0$ and (c) $\Delta=0.01$; (b) and (d): magnification of the figures (a) and (b), respectively.

[Fig. 4(c)], that presents only one vanishing exponent (namely, that related to the direction along the trajectory) [29]. The initial behavior of the $H(t)$ time series can be understood due to the transient time elapsed until the system trajectory settles down on the manifold $\mathcal{M}$. Moreover, two vanishing Lyapunov exponents are related to the phase conjugacies in Eqs. (16) and (17) and are not plotted [23].

IV. MULTISTABILITY

The presence of multiple coexisting attractors, or multistability, is expected in Hamiltonian systems with weak dissipation. In this case, numerical and rigorous analyses point out that there is a large number of coexisting periodic attractors [25]. In the past section we have seen that there is an essentially conservative manifold embedded in the phase space of the system. In the directions transversal to this manifold the dynamics is strongly dissipative, and the trajectories converge fast to this manifold as time goes to infinity. These multiple attractors are limit cycles for $\Delta=0$ and lie on this manifold, their basins extending over the corresponding transversal directions. If $\Delta\neq 0$, these multiple attractors bifurcate into tori, since the conservative manifold $\mathcal{M}$ no longer exists.

If a trajectory were initialized exactly on this invariant manifold it would remain there for all times, without converging to any attractor. With respect to the transversal dissipative direction these curves can be regarded as limit cycles of the system as a whole. Returning to Fig. 2(a), the funnel aspect of the curves is turned into a series of concentric curves if a suitable projection direction is used. In this case the orbits resemble the phase space structure near an elliptic fixed point of a two-dimensional area-preserving system.

For example, a center fixed point of the conservative system (neutrally stable) becomes, with a small amount of dissipation, a stable focus. If this point is in a chain of m periodic islands, it becomes a period-m focus [25,26]. As a general rule, the number of attractors tends to infinity as the dissipation vanishes. For small yet nonzero damping we expect only a finite number of coexisting attractors. This occurs because many periodic orbits (particularly those with high periods) lose their stability in a very rapid way as damping grows up [30].

The fast increase of the number of multiple coexisting attractors of integer periods (in terms of Poincaré maps) is also present when other parameters of the system are varied. For example, keeping the damping fixed in the periodically kicked double rotor [31], there has been found a steep increase in the number of periodic attractors as the forcing decreases to zero [26]. Figure 5 shows the number of periodic attractors we found numerically, with Δ varying eight orders of magnitude. Here the stability of the cycles was obtained numerically: once the numerical integration is started, we wait for the asymptotic state. If this state does not change after a given time interval (*circa* 50 pseudoperiods) we consider that the asymptotic state the system reaches is stable.

As a general trend, the number of coexisting attractors increases exponentially with diminishing Δ, just as expected. The number of attractors N_T, for a given Δ was computed by randomly choosing a large number J of initial conditions in the phase space and following the resulting trajectory a large time, until it closes down on itself (up to a specified small tolerance ε) after m crossings of the Poincaré section. Since the conservative invariant manifold, which exists for $\Delta=0$, is two-dimensional, only periodic orbits with $m=1$ are allowed. Orbits with $m\geqslant 2$ exist only when $\Delta\neq 0$, and do not belong to such conservative invariant manifold. If the orbit fails to close down on itself, we did not consider this trajectory as leading to a periodic orbit. In this case we found an approximation of a period-m attractive orbit, and the number of attractors was computed by summing up all period-m orbits: $N_T=\Sigma_m N_m$. For relatively large Δ (higher than 10^{-5}) we found a power law decrease $N_T\sim\Delta^{-\gamma}$ indicated in Fig. 5(a) by the dotted lines. For $\Delta\lesssim 10^{-5}$ there appears to be a satu-

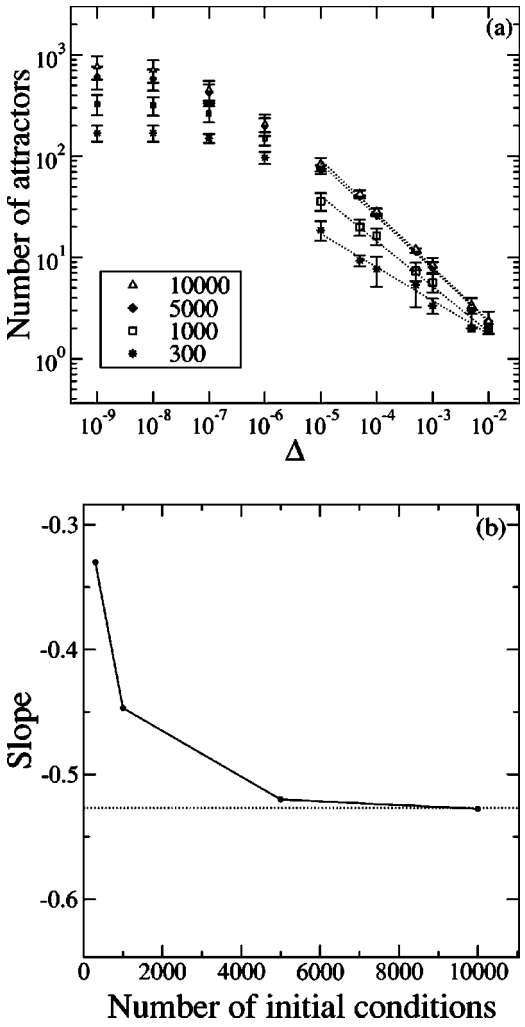

FIG. 5. (a) Number of attractors as a function of the symmetry parameter for a different number of initial conditions. The dashed lines are power-law fits. (b) Variation of the slopes of the power-law fits with the number of initial conditions used.

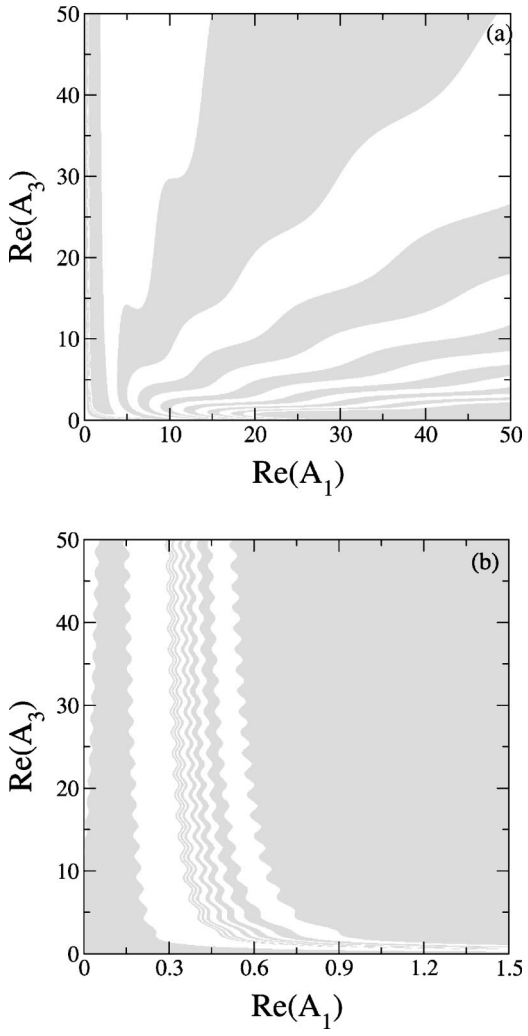

FIG. 6. (a) Basins of coexisting attractors, in the $\mathrm{Re}(A_3)-\mathrm{Re}(A_4)$ projection of the phase space for $\Delta=0$; (b) magnification of the basin structure for small $\mathrm{Re}(A_3)$.

ration of the number of attractors, the error bars being too wide to allow for a reliable fit.

It must be stressed that the numerically determined value of N_T is to be considered actually a lower bound on the total number of periodic attractors, since many orbits have basins of attraction so tiny that their presence cannot be detected unless we use a very fine resolution. This also explains why there is apparent saturation of N_T for very small Δ, since the number of attractors may increase, but at the same time their basins become so small that they cannot be detected. In fact, Fig. 5(a) shows that, while the total number of attractors increases with the number of initial conditions chosen (a consequence of the better resolution achieved with more points to explore), the slopes γ of the power-law fits converge to a value 0.547 ± 0.003 [see Fig. 5(b)].

The basin structure of a weakly dissipative system is thus very complicated, since there is a large number of coexisting stable attractors, each one with its own basin of attraction in a limited phase space region. Even though the phase space dimension can be large, as in this case, there is numerical evidence that the basins of attraction are complexly interwoven [25].

Due to the presence of the conservative manifold in the phase space for $\Delta=0$, with strongly dissipative transversal dynamics, virtually every invariant curve of the conservative manifold is an attractor with respect to the transversal directions, and we label them according to their mean radius $\rho(A_1)$. Since the number of coexisting attractors is typically too large (of the order of hundreds of thousands), it is nearly impossible to get a reasonable plot of individual basins of attraction. However, a glimpse of this structure can be obtained by means of Fig. 6(a), where the union of the basins of various attractors are indicated in the $\mathrm{Re}(A_1)-\mathrm{Re}(A_3)$ projection of the phase space, and corresponding to intervals of the mean radius $\rho(A_1)$. For example, one of the dark strips in Fig. 6(a) refers to the union of the basins for cycles with mean radii within the interval $0<\rho(A_1)<5$, the contiguous white strip to basins for which $5<\rho(A_1)<10$, and so on.

The convoluted nature of the corresponding basin boundaries stripes for small values of $\mathrm{Re}(A_1)$ and $\mathrm{Re}(A_3)$ indicates in fact a highly interwoven basin structure in these regions,

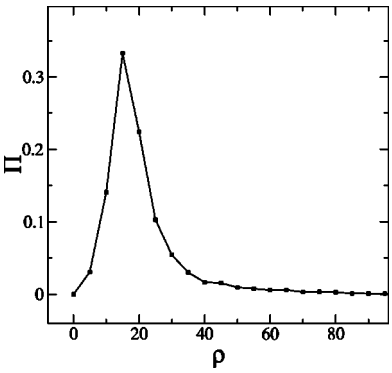

FIG. 7. Probability of reaching a basin of an attractor with a given maximum value of the mean radius $\rho(A_1)$.

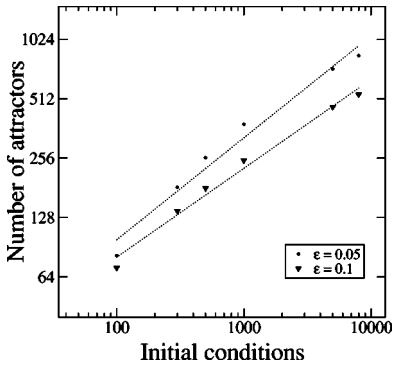

FIG. 8. Number of attractors vs number of initial conditions for two values of the tolerance used.

which holds also for the individual basins themselves. In fact, Fig. 6(b) shows a magnification of such a region, indicating a logarithmic accumulation of the basin stripes towards a vertical line parallel to the axis $\mathrm{Re}(A_1)=0$.

As a consequence of the above reasoning, chaotic attractors are likely to be seldom found in such weakly dissipative systems, for their basins would be too tiny to be detected, in comparison with low-period attractors. However, there are chaotic transients in such systems, present in the basin boundaries, and which are remnants of the homoclinic tangle existing in the conservative case. These chaotic transients, however, do not influence the counting of coexisting attractors.

From Fig. 6 is apparent that the relative areas of the attraction basins are rather different, being distributed in a way numerically shown by Fig. 7, where we have used as an indication of the attractor not its period, but instead the maximum value, $(\rho(A_1))$, of the corresponding periodic orbit. The corresponding probability distribution $\Pi(\rho)$ was computed by distributing a large number of randomly chosen initial conditions in the phase space and determining in what attractor the trajectory settles down. The distribution shows a peak around $|A_1|=20$, indicating the "most probable" periodic orbit in phase space which would contain this value. Such a fact can be observed in Fig. 6(a), where the pieces of projected basins have different areas for different orbits.

At this point, one could argue that, due to the extremely interwoven structure of the attraction basins, very small deviations of a trajectory (particularly if it stays near the basin boundary) would kick us to another basin. This could be a serious drawback of our numerical method to determine a periodic attractor, since it uses a small tolerance ϵ to assess whether or not a given trajectory has closed on itself. In order to give confidence to our method, Fig. 8 shows the variation of the total number of attractors with the total number of initial conditions, for two different tolerances. The number of attractors increases exponentially with initial conditions, which is a simple consequence of the better resolution obtained with more points, permitting us to explore more and more basins of attractions. The slope of this increase is the same for two widely different tolerances. Were the final-state sensitivity so drastic that we would expect dramatic changes by considering small deviations of a trajectory from a tolerance ϵ, the results would not converge as shown by Fig. 8.

V. A LOW-DIMENSIONAL MAPPING

The existence of an invariant manifold $\mathcal{M}$ where the dynamics is nearly conservative, embedded in the phase space of a globally dissipative system, has been suggested for the resonant four-wave interaction. However, the high dimension of the corresponding phase space is an obstacle to a more detailed analysis. For example, one would like to write down an equation for the two-dimensional surface corresponding to $\mathcal{M}$. This is feasible in simpler dynamical systems, where the phase space dimension is small enough to allow the obtention of analytical results.

Since the lowest-dimensional phase space for near-conservative motion is two, the simplest system which exhibits an asymptotically near-conservative dynamics is a two-dimensional weakly dissipative map with a transversal direction with strong dissipation. Furthermore, in order that this area-preserving map is defined on a two-dimensional invariant manifold, the transversal dynamics cannot influence the trajectory in the manifold. We will take, as a representative example of a weakly dissipative map, the Chirikov-Taylor map with a Jacobian slightly smaller than unity [24,28] :

$$x_{n+1} = x_n + y_n + z_n \pmod{2\pi}, \tag{20}$$

$$y_{n+1} = y_n + K \sin[2\pi(x_n + z_n)], \tag{21}$$

$$z_{n+1} = (1-b)z_n, \tag{22}$$

where the standard map is defined the $(x-y)$ plane, and z is the corresponding transversal direction. The dynamics along z is independent from x and y, as required by the requirement that the $z=0$ plane is an invariant manifold. In fact, if we make $z_n=0$ in the above equations, it follows that $z_{n+1}=0$ for all later times. $b \gtrsim 0$ is the dissipation coefficient along the transversal direction. The Jacobian derivative of this model is $\mathcal{J}=1-b$, indicating that, for small b values, this is a globally dissipative map.

If a trajectory starts from an initial condition with nonzero z, i.e., out of the invariant manifold $z=0$, it is typically attracted to the $z=0$ plane, with a constant rate $1-b<0$. An example is depicted in Fig. 9(a), where an $x-y$ projection of the three-dimensional phase space shows closed orbits coming from initial conditions with different values of z. This

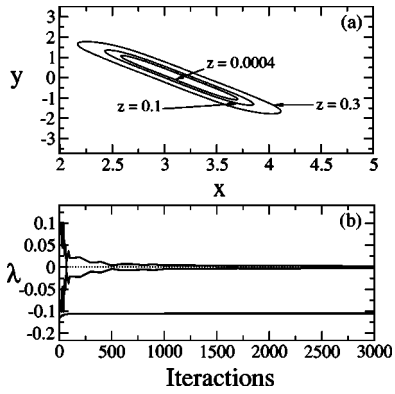

FIG. 9. (a) Projection of the phase space of the three-dimensional mapping showing some closed orbits; (b) time evolution of the Lyapunov exponents of the three-dimensional mapping.

can be interpreted as a result of cross sections, for z variable, of the invariant (KAM) tori which exists in the conservative system ($b=0$). Actually, in the dissipative case these tori no longer exist, the region which they occupy being rather the basin of attraction of a stable focus located at the former elliptic point (see Sec. III). On the other hand, the chaotic motion which is expected for a conservative system like the standard map is readily identified with chaotic transients which precede evolution towards a stable low-period attractor. Figure 9(b) shows the time evolution of the three Lyapunov exponents. The third exponent is negative and is related to the transversal direction, whereas the two largest exponents, after a rapid transient, converge to values related to the dynamics on the $z=0$ plane. If it were strictly conservative, the two largest exponents would sum to zero, due to the area preservation.

VI. CONCLUSIONS

The nonlinear interaction of four waves, in its conservative (Hamiltonian) version, is integrable if there is perfect frequency matching between the waves. The introduction of a small nonzero frequency mismatch breaks down the system integrability and opens the possibility of chaotic dynamics. The addition of dissipative terms to the otherwise conservative model leads to a complex phase space structure, whose main features were the object of this paper. Our results can be summarized as follows.

There coexists a multitude of attractors, their number increasing in a power-law fashion as the symmetry-breaking parameter goes to zero. There exist only limit-cycle attractors, since the invariant manifold is two-dimensional, and their basins of attraction show a highly involved structure with an incursive character, which is more evident for low values of the wave amplitudes. The presence of chaotic attractors is not possible in this case, but this does not preclude the existence of chaotic transient dynamics.

We have numerically observed that the system trajectories for the $\Delta=0$ case, albeit belonging to a high-dimensional phase space, are asymptotically converging to a two-dimensional invariant manifold in which the dynamics is conservative. This fact effectively reduces the number of degrees of freedom necessary to give a dynamical characterization of the wave-interaction problem. These properties can also be found in simpler dynamical systems, and we have introduced a three-dimensional mapping which share many of the properties of the physical system we are considering in this paper. We claim that our results are thus quite general, and are present in a wide variety of similar wave-interaction models.

ACKNOWLEDGMENTS

This work was made possible through partial financial support from the following Brazilian research agencies: CNPq and CAPES.

[1] B. Coppi, M. N. Rosenbluth, and R. N. Sudan, Ann. Phys. (N.Y.) **55**, 207 (1969).
[2] J. Weiland and H. Wilhelmsson, *Coherent Nonlinear Interaction of Waves in Plasmas* (Pergamon, Oxford, 1977).
[3] J. M. Wersinger, J. M. Finn, and E. Ott, Phys. Rev. Lett. **44**, 453 (1980).
[4] J. M. Wersinger, J. M. Finn, and E. Ott, Phys. Fluids **23**, 1142 (1980).
[5] E. Ott, Rev. Mod. Phys. **53**, 655 (1981).
[6] Y. S. Dimant, Phys. Rev. Lett. **84**, 622 (2000).
[7] W. L. Kruer, *The Physics of Laser Plasma Interactions* (Addison-Wesley, Redwood City, CA, 1988).
[8] A. C.-L. Chian, S. R. Lopes, and M. V. Alves, Astron. Astrophys. **290**, L13 (1994).
[9] A. C.-L. Chian and F. B. Rizzato, J. Plasma Phys. **51**, 61 (1994).
[10] Y. R. Shen, *The Principles of Nonlinear Optics* (Wiley, New York, 1984).
[11] P. Fischer, D. S. Wiersma, R. Righini, B. Champagne, and A. D. Buckingham, Phys. Rev. Lett. **85**, 4253 (2000).
[12] A. Rundquist, C. G. Durfee III, Z. Chang, C. Herne, S. Backus, M. M. Murnane, and H. C. Kapteyn, Science **280**, 1412 (1998).
[13] S. M. Spillane, T. J. Kippenberg, and K. J. Vahala, Nature (London) **415**, 621 (2002).
[14] L. Deng, E. W. Hagley, J. Wen, M. Trippenbach, Y. Band, P. S. Julienne, J. E. Simsarian, K. Helmerson, S. L. Rolston, and W. D. Phillips, Nature (London) **398**, 218 (1999).
[15] A. Picozzi and M. Haelterman, Phys. Rev. Lett. **86**, 2010 (2001).
[16] A. Picozzi and M. Haelterman, Phys. Rev. Lett. **88**, 083901 (2002).
[17] D. A. Russell and E. Ott, Phys. Fluids **24**, 1976 (1981).
[18] C. Meunier, M. N. Bussac, and G. Laval, Physica D **4**, 236 (1982).
[19] R. Sugihara, Phys. Fluids **11**, 178 (1968).

[20] K. S. Karplyuk, V. N. Oraevskii, and V. P. Pavlenko, Plasma Phys. **15**, 113 (1973).
[21] F. J. Romeiras, Phys. Lett. **93A**, 227 (1983).
[22] A. C.-L. Chian, S. R. Lopes, and J. R. Abalde, Physica D **99**, 169 (1996).
[23] R. Pakter, S. R. Lopes, and R. L. Viana, Physica D **110**, 277 (1997).
[24] A. J. Lichtenberg and M. A. Lieberman, *Regular and Stochastic Motion* (Springer-Verlag, New York, 1983).
[25] U. Feudel and C. Grebogi, Chaos **7**, 597 (1997).
[26] U. Feudel, C. Grebogi, L. Poon, and J. A. Yorke, Chaos, Solitons Fractals **9**, 171 (1998).
[27] Y. S. Dimant and R. N. Sudan, Bull. Am. Phys. Soc. **44**, 1119 (1999).
[28] B. Chirikov, Phys. Rep. **52**, 263 (1979).
[29] E. Ott, *Chaos in Dynamical Systems*, 2nd ed. (Cambridge University Press, Cambridge, England, 2002).
[30] U. Feudel, C. Grebogi, B. Hunt, and J. A. Yorke, Phys. Rev. E **54**, 71 (1996).
[31] C. Grebogi, E. J. Kostelich, E. Ott, and J. A. Yorke, Phys. Lett. A **118**, 498 (1986).